IFAI Geosynthetics Conference
Feb. 10-13, 2019 | Houston, TX USA

Development of a Shear Test for Unreinforced and Geosynthetic-Reinforced Hot Mix Asphalt

L. Yang, M.Sc.,[1] G. H. Roodi, Ph.D.,[2] and J. G. Zornberg, Ph.D., P.E.[3]

[2]Department of Civil, Architectural, and Environmental Engineering, The University of Texas at Austin, 301 E. Dean Keeton St. Stop C1792, Austin, TX 78712; e-mail: hroodi@utexas.edu

ABSTRACT

Inclusion of geosynthetics within hot mix asphalt layers has been reported to be an effective technique to enhance the performance of pavements. The experimental study presented in this paper introduces a new focus for evaluation of unreinforced and geosynthetic-reinforced asphalt specimens. Specifically, a new shear test was developed to evaluate the geosynthetic benefits in geosynthetic-reinforced asphalt specimens subjected to shearing along the cross-geosynthetic direction. In the developed shear test, the cross section of the specimen can be subjected to monotonic or cyclic shear loading. The cracks are expected to initiate and propagate along the cross-geosynthetic direction as the number of loading cycles increases. Following the development of the test equipment, a rigorous test procedure and data analysis protocol was adopted to evaluate unreinforced and geosynthetic-reinforced asphalt specimens. An experimental program was then conducted to compare responses of a control (unreinforced) asphalt specimen with an asphalt specimen that was reinforced using a polyester geosynthetic in its middle. Specifically, the control and geosynthetic-reinforced specimens were tested under monotonic and sinusoidal shear loading. The obtained test results underscored that the geosynthetic reinforcements can effectively enhance the performance of the asphalt under monotonic shear as well as cyclic shear loading. Specifically, the main benefit from geosynthetic inclusion was found in the enhanced residual shear resistance and increased energy absorbed by the geosynthetic-reinforced specimen.

INTRODUCTION

The wide range of distresses in pavements requires intensive studies to pinpoint the causes of the distresses and invest in effective solutions to mitigate pavement problems. Typical stress state in pavement surface layer subjected to traffic loading is illustrated in Figure 1 (Carvalho and Schwartz 2013). The experimental studies regarding pavement surface layer often focus on combinations of the stress components illustrated in Figure 1 using a wide range of test setups.

The experimental studies on the performance of reinforced asphalt have used various loading mechanisms. A wide range of studies have investigated the debonding at the interface between the geosynthetic and asphalt (e.g., Roodi et al. 2017). Kumar and Saride (2018) conducted a direct tensile test on reinforced and unreinforced asphalt specimens under different temperatures using various types of geosynthetics. Montestruque et al. (2004) designed and conducted dynamic beam fatigue tests to evaluate the performance of the reinforced asphalt beam specimens. Khodaii et al. (2009) also conducted beam fatigue tests loaded using a circular steel plate to study the

effectiveness of geosynthetic inclusion and its position on the crack development and plastic deformation. They reported increased cracking and rutting resistance in the geosynthetic-reinforced asphalt specimens as compared to unreinforced specimens (Khodaii et al. 2009). Small-scale wheel tracking tests were conducted by Montestruque et al. (2012). They used a displacement-controlled wheel tracking test to evaluate an anti-reflective composite interlayer system. Montestruque et al. (2012) have proposed the composite system including a combination of a stress relief asphalt layer and a reinforcing geogrid as an efficient solution for mitigation of reflective cracking. Pasquini et al. (2015) have designed a specific moving-wheel experimental system to simulate reflective crack propagation under loading.

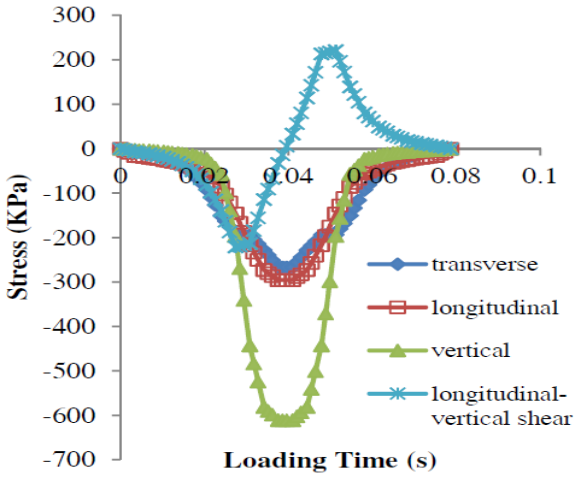

Figure 1. Stress components of one point in pavement (from Carvalho and Schwartz (2013))

A new shear test setup was developed in this study to evaluate asphalt specimens subjected to pure shear and to determine geosynthetic benefits in geosynthetic-reinforced asphalt specimens subjected to pure shearing in the cross-geosynthetic direction. The developed test can be used in monotonic or cyclic loading schemes. Therefore, this test can also be categorized as a fatigue test that tests the shear properties of the unreinforced or geosynthetic-reinforced asphalt specimens by applying sinusoidal displacement loads. In the developed shear test, the cross section of the specimens is subjected to be pure shear and shear cracks are expected to develop along the cross-geosynthetics direction with the increasing displacement or increasing number of loading cycles.

DEVELOPMENT OF SHEAR TEST

A brick shape asphalt specimen was glued onto steel plates that on both sides using epoxy. The steel plates were positioned with a small gap so that one side of the asphalt specimen can be sheared versus the other side along the cross section passing through the gap. The asphalt specimen along with the attached steel plates were mounted onto a conventional loading frame that has been typically used for cyclic triaxial test. One side of the specimen was secured on a rigid base and the other side was loaded vertically while hanging in the air.

Initially, a rubber bed was used under the loading side of the specimen and the shear test was designed to be load-controlled with sinusoidal waveform. However, it was found that the

responses under the load-controlled test setup was highly sensitive to the characteristics of the rubber bed. Therefore, the loading system was changed to displacement-controlled.

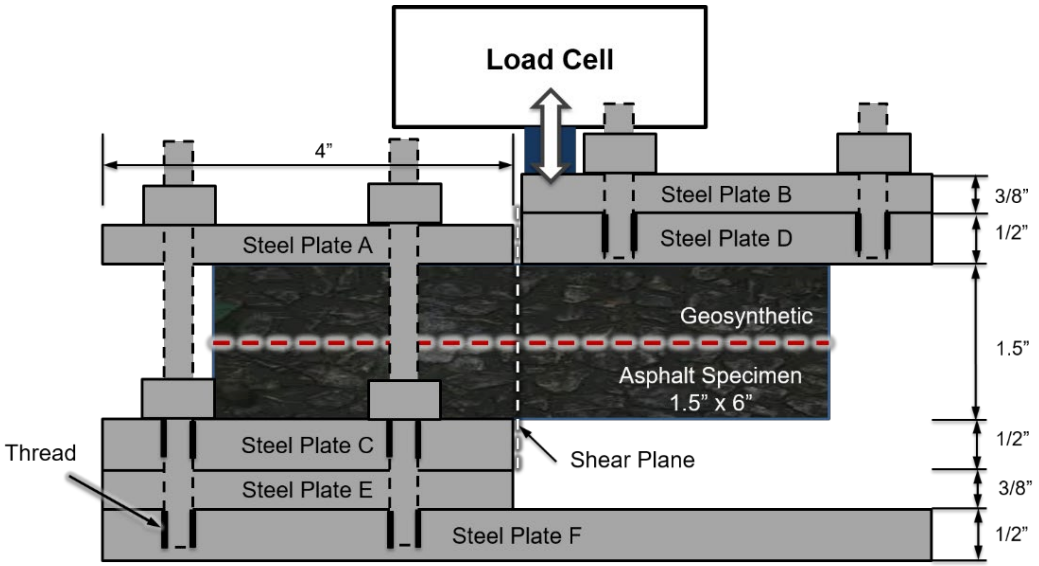

Figure 2. Sketch of the developed shear test setup

The finalized test set setup is shown in Figure 2. The test setup consisted of 6 pieces of steel plates (Steel Plates A to F), steel rods, nuts and washers. The asphalt concrete specimen was designed to be glued onto Steel Plates C and D using epoxy. The left half of the specimen was secured between Steel Plates A and C and was not expected to move during the shear test. Steel Plate C was firmly secured using threaded steel rods and nuts into the bottom Steel Plate F to ensure the left half of the specimen remain fixed. Steel Plate A secured the top surface of the left half asphalt specimen without inducing compression to the asphalt. This plate was used as an additional support to prevent uplift of the left half of the specimen. The gap between the fixed half (on the left in Figure 2) and the loaded half (on the right in Figure 2) of the setup was 3 mm. The dimensions of the major parts of the test setup and asphalt specimen are displayed in Figure 2. As previously noted, this test setup was designed to apply displacement-controlled shear load. The loading rod was attached onto Steel Plate B on the edge of the gap on top of the right half of the specimen. The test setup allowed applying controlled monotonic and cyclic displacements in the vertical direction. The right half of the specimen, glued on its top surface to Steel Plate D, was expected to move vertically while the left half of the specimen remained stationary.

The loading machine, and data acquisition and control systems were manufactured by GCTS and have been originally designed for the cyclic triaxial test. Vertical load and vertical displacements were measured using a load cell and a linear variable differential transformer (LVDT) connected to the loading rod. An additional setup was adopted to capture images of the specimen as the test progress. The captured images were then used to track the development of cracks in the unreinforced and geosynthetic-reinforced asphalt specimens. Figure 3. (a) shows various components of the test setup and Figure 3. (b) shows the asphalt specimen along with the steel plate's assembly mounted onto the loading frame.

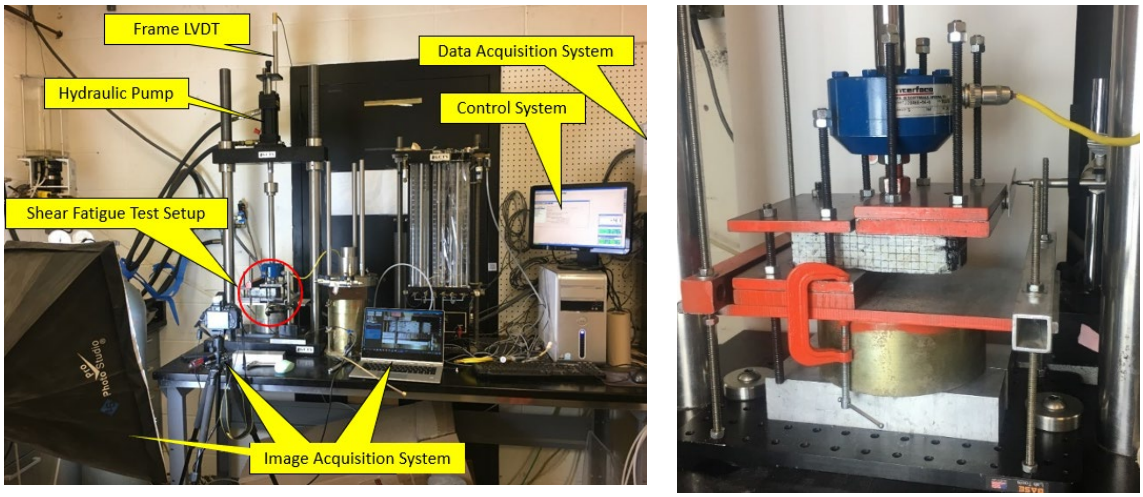

(a) b)

Figure 3. Test setup for the developed shear test: (a) various components of the test setup; (b) asphalt specimen and steel plates assembly

TEST DESIGN

Two loading schemes were adopted in the experimental program including a monotonic test and a sinusoidal cyclic test. The monotonic shear test involved displacement-controlled loading of the right half of the specimen using a constant vertical downward displacement rate of 7.62 mm/min. The data points were recorded every 0.025 sec from the load cell, frame LVDT and lateral LVDT. Findings from the monotonic tests were used along with several trials of cyclic tests to optimize the configurations for cyclic tests. Specifically, amplitude and frequency of sinusoidal cyclic load were changed to obtain a configuration that would result in the fatigue failure of the unreinforced and geosynthetic-reinforced asphalt specimens within a reasonable number of loading cycles. The finalized cyclic shear loading scheme consisted of 4 phases of displacement-controlled sinusoidal loading with increasing displacement amplitude between phases. The frequency of the input sinusoidal displacements was 1 Hz for all 4 phases and the peak-to-peak amplitudes were 0.75 mm, 1.0 mm, 1.5 mm, and 2.0 mm, for Phases 1 to 4, respectively. The number of cycles was 5,000 for each phase. The total duration of the cyclic shear test was about 6 hours.

DATA ANALYSIS

The main data and parameters that were used in the analysis of the test results obtained from the developed shear test are explained here.

Monotonic shear test. The analysis of the monotonic test results was based on the following data:

1) Normalized load-displacement data, which was obtained by normalizing the measured load by the section area of the asphalt specimen plotted versus the vertical displacement;

2) Normalized maximum load, which was obtained by dividing the maximum load by the section area of the specimen;

3) Shear strain at maximum load, which was defined as the displacement corresponded to the maximum load divided by the thickness of the specimen;

4) Normalized fracture energy, which was defined as the energy required to fracture the specimen and was calculated by dividing the area under the vertical load-vertical displacement curve from beginning of the test to the peak load, referred to as the fracture energy (in N • mm), by the cross section of the specimen (in mm^2);

5) Normalized cumulative energy, which was defined as the cumulative energy absorbed by the specimen during the monotonic test normalized by the section area of the specimen. Apparently, this parameter was expected to have an ascending trend throughout the test.

Cyclic shear test. The analysis of the cyclic test results was based on the following data:

1) Normalized load decline curve, which was obtained by normalizing the measured load by the section area of the asphalt specimen plotted versus the number of loading cycles;

2) Normalized maximum load for each phase, which was obtained by dividing the maximum load within the 1st cycle of each phase by the cross-section area of the specimen;

3) Crack resistance index for each phase, which was obtained using a linear regression to relate the natural logarithm of the normalized peak loads and the natural logarithm of the number of loading cycles. The crack resistance index describes the rate of load reduction in the normalized load decline curve. The fitting curve to the normalized load decline curve can be described as follows:

$$lnP = (0.075\beta - 1)lnN + \alpha \quad (1)$$

where, N = number of loading cycle, P =normalized peak load in each loading cycle, $\alpha =$ the natural logarithm of the normalized maximum load; and β is the crack resistance index. The crack resistance index was calculated for each phase of the cyclic shear tests;

4) Normalized residual load for each phase, which was obtained by dividing the residual peak load measured in the last loading cycle of each phase by the section area of the specimen;

5) Normalized cumulative energy, which was defined as the cumulative energy absorbed by the specimen during the cyclic test normalized by the section area of the specimen.

EXPERIMENTAL RESULTS

Two monotonic tests and two cyclic tests were conducted on unreinforced and geosynthetic-reinforced asphalt specimens using the develop test setup. The obtained results were compared to evaluate potential benefits from geosynthetic reinforcement of asphalt.

Material properties and specimens. The asphalt binder used in this study was PG 76-22. The aggregates used for asphalt mixture were sieved from both coarse and fine aggregates. The aggregates mixture followed TxDOT Type D gradation curve. The asphalt mixture consisted of 6.5% binder (PG 76-22) and 93.5% of aggregate by weight. The tack coat used in this study was CHFRS-2P, which is a cationic, high float, rapid setting emulsion that has a comparatively high viscosity and also contains polymers. The tack coat was applied to the specimen at a rate of approximately 0.121 to 0.145 gal/yd^2. The geosynthetic product used in this study was HaTelit® C40/17, which is a polyester geogrid manufactured by Huesker. The asphalt mixture was compacted in a 6-in.-diameter cylindrical mold and trimmed into a 3 in. wide by 1.5 in. thick asphalt specimen. The asphalt specimens are either unreinforced (CTRL) or reinforced with HaTelit® C40/17 (MC40/17) in the middle.

Monotonic tests. The normalized load – displacement data for monotonic tests are presented in Figure 4. Evaluation of the data presented in this figure indicates that the geosynthetic-reinforced specimen not only showed a higher peak load per section area than the unreinforced specimen, but also it had a higher stiffness. This observation indicates that the geosynthetic reinforcement was engaged in providing additional shear resistance to the specimen from the beginning of the test. The peak load in both cases occurred at approximately 2 mm of vertical displacements, which probably corresponded to the yielding of the asphalt in both specimens. However, an important contribution from geosynthetic reinforcement was observed after the peak load. Specifically, while the residual shear resistance in the unreinforced specimen was found to be approximately zero, the geosynthetic-reinforced specimen was found to have significantly larger residual shear resistance, which extended to comparatively large shear strain values.

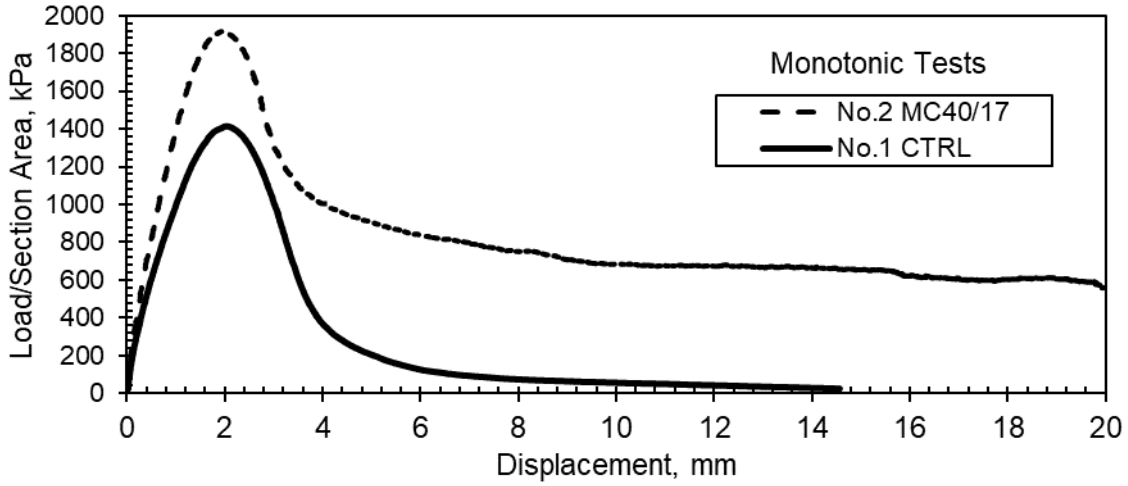

Figure 4. Normalized load – displacement curves for monotonic tests

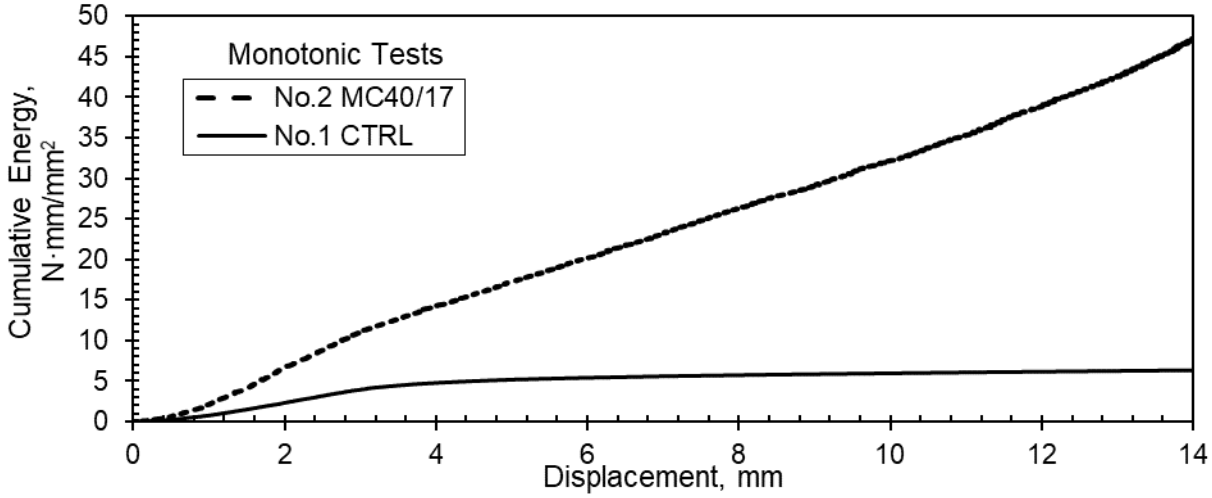

Figure 5. Normalized cumulative energy for monotonic tests

The normalized cumulative energy observed by each specimen in the monotonic tests is presented in Figure 5. This data was obtained by calculating the cumulative area underneath the load-displacement curve presented in Figure 4. The difference between the normalized cumulative

energies was not significant in the initial 1 mm displacement. However, the different slopes observed in the data started at higher shear displacements indicates significant difference in the absorbed energies by the unreinforced and the geosynthetic-reinforced specimens. This finding underscores contribution of the geosynthetic reinforcement in the shear resistance. The cumulative energy in the monotonic test on the unreinforced specimen approaches a constant value at the end of the test because its residual load was zero. However, the cumulative energy for the reinforced specimen continued increasing towards the end of the test, suggesting that the reinforcement in the asphalt concrete was still absorbing energy at larger displacement (or shear strain level) without breakage. This observation suggests that geosynthetic-reinforced asphalt layers continue to sustain shear resistance even after the asphalt is fully cracked.

The parameters of the monotonic tests are summarized in Table 1. This table also present the ratio between the values obtained in the reinforced specimens to those obtained in the unreinforced specimen. Evaluation of these ratios indicates that the most significant benefit from geosynthetic inclusion can be observed in the parameter that corresponds to the total absorbed energy by the specimen after breakage of the asphalt (i.e., at comparatively large displacements).

Table 1. Summary of parameters obtained in monotonic tests

#	Description	Normalized maximum load, kPa	Shear strain at maximum load, %	Normalized fracture energy, $N \cdot mm/mm^2$	Normalized cumulative Energy at 14 mm displacement, $N \cdot mm/mm^2$
1	Unreinforced Specimen	1,414	4.8%	2.3	6.3
2	Geosynthetic-reinforced Specimen	1,918	5.7%	6.4	47
Ratio (Reinforced to Unreinforced values)		1.35	1.19	2.78	7.46

Cyclic tests. The normalized load decline curves for all phases of the cyclic shear tests are presented in Figure 6. In Figure 6. (a), this data is presented for all phases using a linear scale for number of loading cycles. In Figures 6. (b) to (e), the normalized load decline curves are presented for individual phases using a logarithmic scale for number of loading cycles. The normalized load decline curve in the linear scale (Figure 6. (a)) provides a clear presentation for comparisons of the response observed from the unreinforced and the reinforced specimens throughout the entire tests. The normalized load in the reinforced specimen was found to be higher than that of the control specimen throughout the entire 20,000 cycles. Specifically, both normalized maximum and normalized residual loads were found to be higher in the reinforced specimen than in the unreinforced specimen.

The normalized load of the specimens was plotted in the semi-log scale for each of the phases to better demonstrate the maximum and residual loads for the specimens (Figures 6. (b) to (e)). The normalized maximum and residual loads obtained for the unreinforced and reinforced specimens in each phase along with the ratio of these values for the reinforced specimen to that in the unreinforced specimen are presented in Table 2. Consistent with the observation in the monotonic tests, in all phases the geosynthetic reinforcement was found to have a higher impact on the residual shear resistance than the maximum shear resistance. Furthermore, the impact of geosynthetic on both maximum and residual shear resistance was found to be more significant in the latter phases of the cyclic test than in the initial phase. This findings indicates comparatively higher benefit of geosynthetic after cracks have developed in the asphalt in the initial phase of the tests.

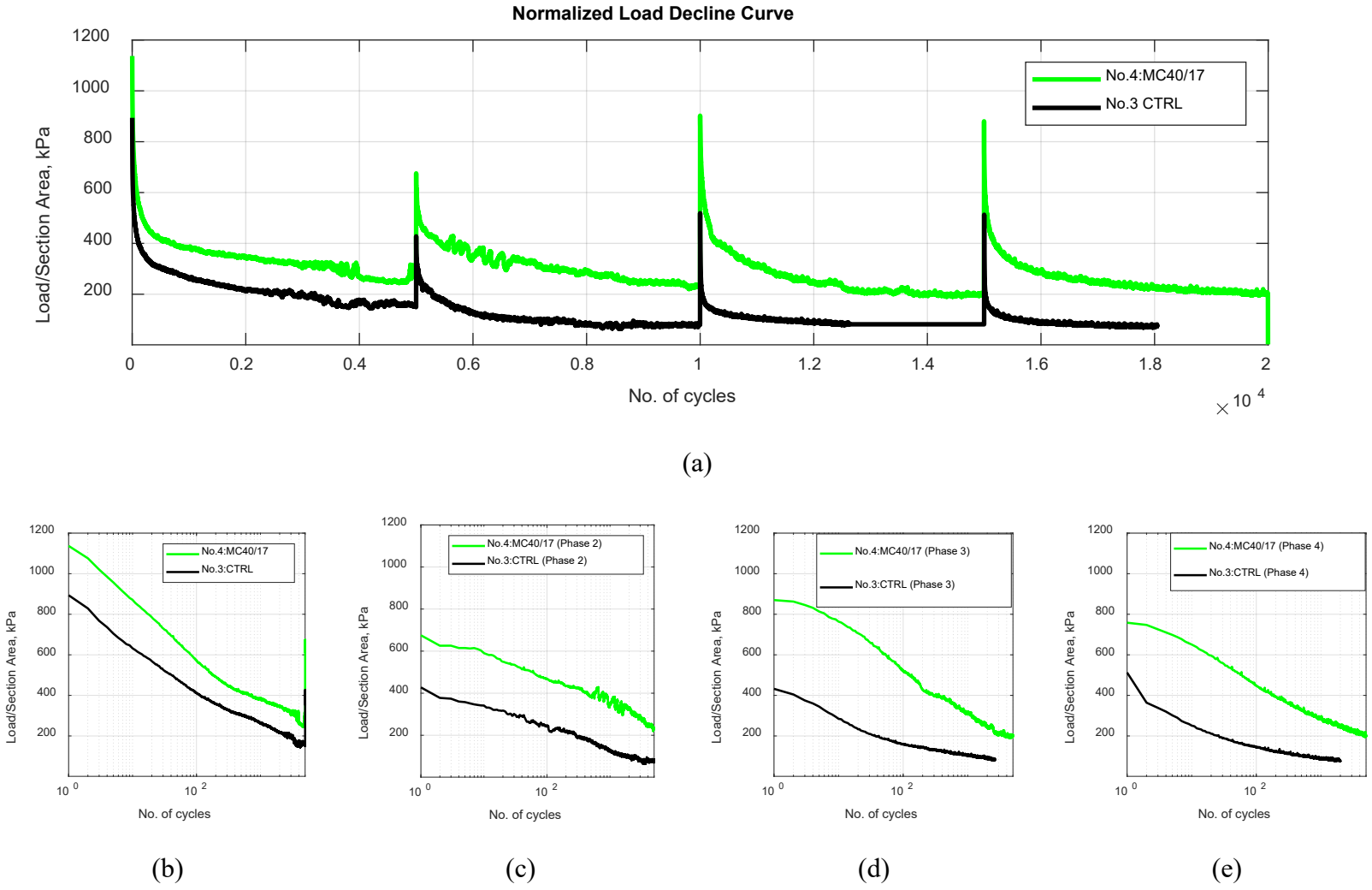

Figure 6. Normalized load decline curves for cyclic tests: (a) all phases in linear scale; (b) Phase 1 in semi-log scale; (c) Phase 2 in semi-log scale; (d) Phase 3 in semi-log Scale; (e) Phase 4 in semi-log Scale

The crack resistance index (β in Equation (1)) was also calculated for all phases of the cyclic tests on the reinforced and unreinforced specimens. This data is also presented in Table 2. The crack resistance index values were found to be similar in all phases and for both reinforced and unreinforced specimens.

Table 2. Summary of parameters obtained in cyclic tests

Description	Peak Load/Section Area, kPa				Residual Load/Section Area, kPa				Crack Resistance Index, β			
	P1	P2	P3	P4	P1	P2	P3	P4	P1	P2	P3	P4
Unreinforced Specimen	894	428	519	513	156	82	82	73	9.9	9.1	10.5	10.6
Geosynthetic-reinforced Specimen	1,137	675	902	880	305	234	199	196	10.7	10.8	9.8	10.6
Ratio (Reinforced to Unreinforced values)	1.27	1.58	1.74	1.72	1.96	2.85	2.43	2.68	1.08	1.19	0.93	1.00

The normalized cumulative energy absorbed by each specimen in the cyclic tests is presented versus the number of cycles in Figure 7. The energy that both specimens absorbed increased with the increase in the number of loading cycles. The absorbed energies in the unreinforced and reinforced specimens were comparatively close in the first phase of the test (i.e., at number of loading cycles less than 5,000). However, the reinforced specimen absorbed significantly higher energy than the unreinforced specimen in latter phases (i.e., at number of loading cycles that exceeds 5,000). None of the cumulative energy curves reached a plateau because none of the specimens reached to zero resistance shear at the end of the tests.

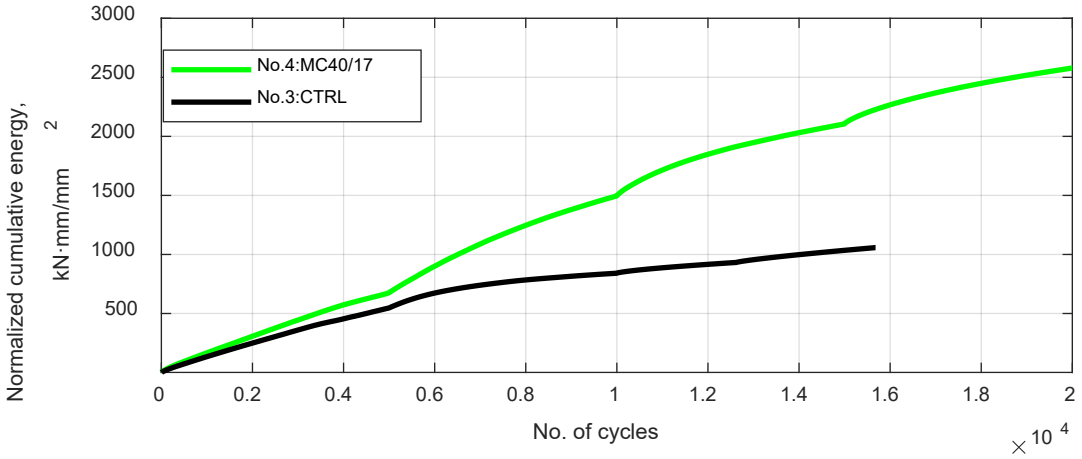

Figure 7. Normalized cumulative energy in cyclic tests

SUMMARY AND CONCLUSION

A new test setup was developed to evaluate performance of unreinforced and geosynthetic-reinforced asphalt specimens under shear loading of their cross-sections. In this test setup, a brick shape asphalt specimen is secured using steel plate's assembly. One half of the specimen remains fixed and the other half is subjected to monotonic or cyclic loading. Various components of the test setup was carefully designed and a rigorous test procedure and data analysis was adopted. The

developed setup allows evaluation of the performance of geosynthetic-reinforced and unreinforced asphalt specimens under monotonic shear loading as well as cyclic shear fatigue loading.

Two geosynthetic-reinforced and two unreinforced asphalt specimens were tested under monotonic shear and cyclic shear fatigue loadings. Significant benefits from geosynthetics were observed in both monotonic and cyclic shear tests. Specifically, the maximum shear resistance was found to enhance at least 30 percent in the geosynthetic reinforced specimen. Nevertheless, geosynthetic inclusion resulted comparatively higher improvements in the residual shear resistance and the absorbed energy by the specimens. After the peak loads in the monotonic tests, the load in the reinforced specimen dropped more gradually than the control specimen. The reinforced specimen sustained a considerably high residual shear resistance at comparatively high shear displacements. This finding suggests that geosynthetic-reinforced asphalt layers may continue to sustain the shear resistance even after the asphalt is fully cracked.

The energy absorbed by the geosynthetic-reinforced and unreinforced asphalt specimens were similar at small displacements in the monotonic test. This energy was also similar for both specimens under comparatively small loading amplitude in the monotonic tests. However, in both loading schemes, the cumulative energy absorbed by the geosynthetic-reinforced specimen was found to be significantly higher than the unreinforced specimen when comparatively higher displacements were imposed.

Overall, the developed shear test and the corresponding test design and data analysis were found to be particularly suitable to evaluate the difference between the performance of unreinforced and geosynthetic-reinforced asphalt specimen subjected to shear loading.

ACKNOWLEDGMENT

The authors acknowledge the support received from Huesker, Inc. The help of Hamza Jaffal, Federico Castro, Ramez Hajj, and Chian Hen Tam is also greatly appreciated.

REFERENCES

Carvalho, R.L., and Schwartz, C.W. (2013). The importance of simulating moving wheel loads in the mechanistic analysis of permanent deformations in flexible pavements, *Airfield and Highway Pavement 2013: Sustainable and Efficient Pavements*, Los Angeles, CA, USA, 1156-1166.

Khodaii, A., Fallah, S., and Nejad, F.M. (2009). Effects of geosynthetics on reduction of reflection cracking in asphalt overlays, *Geotextiles and Geomembranes*, Elsevier, 27(1):1-8.

Kumar, V.V., and Saride, S. (2018). Evaluation of cracking resistance potential of geosynthetic reinforced asphalt overlays using direct tensile strength test, *Construction and Building Materials,* Elsevier, 162:37-47.

Montestruque, G., Bernucci, L., Fritzen, M., and da Motta, L.G. (2012). Stress relief asphalt layer and reinforcing polyester grid as anti-reflective cracking composite interlayer system in pavement rehabilitation, *7th RILEM Conference on Cracking in Pavements*, Portugal, Springer, 1189-1197.

Montestruque, G., Rodrigues, R., Nods, M., and Elsing, A. (2004). Stop of reflective crack propagation with the use of PET geogrid as asphalt overlay reinforcement, *5th RILEM Conference on Cracking in Pavements*, Limoges, France, RILEM Publications S.A.R.L., 231-238.

Pasquini, E., Pasetto, M., and Canestrari, F. (2015). Geocomposites against reflective cracking in asphalt pavements: Laboratory simulation of a field application, *Road Materials and pavement Design,* Taylor and Francis, 16(4):815-835.

Roodi, G.H., Morsy, A.M., and Zornberg, J.G. (2017). Experimental evaluation of the interaction between geosynthetic reinforcements and hot mix asphalt, *International Conference on Highway Pavement &* Airfield *Technology*, ASCE, Philadelphia, PA, 428–439.